to attenuate hepatic and cardiac TNF-α synthesis in splanchnic artery reperfusion injury or lethal endotoxemia.[10,11] We[12] and LaCroix et al[13] have demonstrated that VS induces expression of tissue inhibitor of MMP (TIMP)-1 and reduces active MMP-9 in ischemic myocardium. Although these findings suggest that VS favorably modulates the inflammatory reactions in MI, the effects of VS on inflammatory responses including the expression of cytokines and MMPs as well as its association with the inflammatory cell infiltrations have not been investigated in the setting of MI.

Long-term VS requires permanent implantation of the entire stimulating system.[3,4] However, hemodynamically unstable patients with acute MI are poor surgical candidates. On the other hand, early brief VS via an intravascular[14] or a transcutaneous approach[11] without compromising the hemodynamic conditions would be feasible in acute clinical settings. Taking all these together, the objective of this study was to investigate the effects of early short-term VS on LV function and myocardial structural remodeling in a rabbit model of reperfused MI and their association with acute inflammatory reactions.

Methods

Animals

We used a total of 56 Japanese white rabbits in this study (male, 2.5 to 3.0 kg). The investigation conforms with the *Guide for the Care and Use of Laboratory Animals* published by the US National Institutes of Health (NIH Publication No. 85-23, revised 1996). All protocols were approved by the Animal Subjects Committee of the National Cardiovascular Center (approval number: 8042). Rabbits were assigned to the MI group (left coronary artery occlusion and reperfusion only; n = 24), MI-VS group (left coronary artery occlusion and reperfusion plus early short-term VS; n = 22), and normal control (NC) group (no treatment; n = 10).

Implantation of Vagal Nerve Electrode

Rabbits in the MI-VS group were implanted with vagal nerve electrodes. Under general anesthesia (sodium pentobarbital, 35 mg/kg^{-1}) and mechanical ventilation, a pair of polyurethane-coated stainless steel wires for electrical stimulation was looped around the right vagal nerve in the neck region.[3] The electrode wires were tunneled beneath the skin, exited in the midscapular area, and connected to a radio-controlled pulse generator (SRG-3100, Nihon Kohden, Japan) placed in a nylon jacket. Rabbits in the MI group underwent sham surgery without implanting the electrode. The animals were allowed to recover for at least 1 week before induction of MI (Fig. 1).

Induction of MI

MI was induced in rabbits of the MI and MI-VS groups (Fig. 1). Under general anesthesia (sodium pentobarbital, 35 mg/kg^{-1}) and mechanical ventilation with room air, a left thoracotomy was performed. A 4-0 proline suture was passed around the circumflex coronary artery, and a snare was formed by passing the ends of the thread through a small vinyl tube.[12] Electrodes to record surface electrocardiogram were implanted subcutaneously. The circumflex tourniquet was tightened to completely stop blood flow

as demonstrated by both electrocardiogram changes and visual blanching of the myocardium. In the MI-VS group, we started vagal nerve stimulation immediately after coronary occlusion using rectangular pulses of 1-ms duration at 20 Hz for 10 seconds every minute.[3] We adjusted the amplitude of the pulse in each animal to reduce heart rate (HR) by 10% from baseline value. Consequently, the amplitudes ranged from 2 to 8 V. In a preliminary study, we confirmed that VS at this intensity did not alter feeding behavior and did not evoke any sign of pain reaction. After 60 minutes of coronary occlusion, the tourniquet was released, allowing reperfusion in both groups. The chest wall was then closed, and the animal was allowed to recover.

After recovery from anesthesia of MI surgery, we checked HR response to VS in MI-VS rabbits by monitoring electrocardiogram at least twice per day under conscious condition. We readjusted the intensity of VS if necessary, because the response varied from day to day in an individual rabbit.

Experimental Protocols

We performed 2 studies (Fig. 1). In study 1, VS was continued for 24 hours in MI-VS rabbits, and the effects of VS on myocardial inflammatory reactions at 24 hours after coronary reperfusion were examined because myocardial expression of TNF and MMP-9 as well as infiltration of neutrophil have been shown to peak at around 24 hours after myocardial ischemia reperfusion.[15] In study 2, VS was continued for 3 days in MI-VS rabbits, and LV function and structure were examined at 8 weeks after coronary reperfusion.

Study 1: Acute Phase after MI

Study 1 consisted of 3 groups of rabbits: MI (n = 8), MI-VS (n = 8), and NC (n = 3). At 24 hours after coronary reperfusion, animals in the MI and MI-VS groups were euthanized and whole hearts were harvested.

Western Blot. Myocardial tissue sample obtained from the LV lateral wall (infarct region in MI and MI-VS rabbits) was homogenized in RIPA lysis buffer (Rockland, Gilbertsville, PA) containing proteinase inhibitor (Complete Mini, Roche, Basel, Switzerland). The homogenate was centrifuged at 4 °C at 2000g for 10 minutes and the resultant supernatant was further subjected to centrifugation at 12,000g for 20 minutes. Protein concentration of each supernatant sample was determined using a DC Protein assay kit (BioRad Hercules, CA).

Samples containing equal amounts of protein (25 μg) were separated on 15% sodium dodecyl sulfate polyacrylamide gel electrophoresis gel (Bio-Rad) and transferred onto Immobilon-P membrane (Millipore, Billerica, MA). After blocking the membranes with BlockAce (Dainippon Pharmaceutical, Japan), TNF-α was detected with polyclonal antibody for TNF-α (sc-1348, Santa Cruz, CA) and donkey-anti-goat HRP (sc-2020, Santa Cruz). Interleukin-1β (IL-1β) was detected with polyclonal antibody for IL-1β (LS-C7719, LifeSpan Biosciences, Seattle, WA) and goat-anti-rabbit HRP (sc-2004, Santa Cruz). MMP-1, MMP-7, MMP-8, and β-actin were detected using monoclonal antibodies for MMP-1 (F-67, Daiichi Fine Chemical, Japan), MMP-7 (F82, Daiichi Fine Chemical), MMP-8 (F-83, Daiichi Fine Chemical), and β-actin (sc-47778, Santa Cruz), respectively, and goat-anti-mouse HRP (sc-2005, Santa Cruz). Protein bands were visualized with ECL Plus (GE Healthcare, UK), and analyzed using a densitometric analysis software (CS Analyzer 3.0, ATTO, Japan). Band densities were standardized to β-actin, and presented as percent
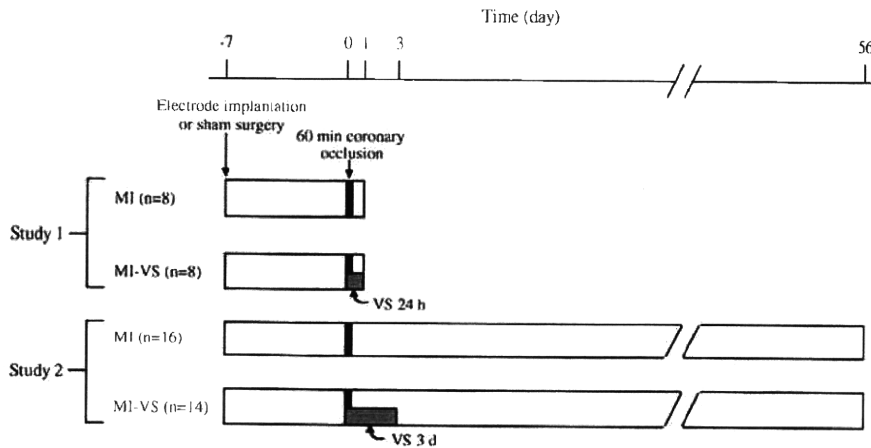
Fig. 1. Schematic representation of the protocols of Study 1 (acute phase myocardial infarction and reperfusion) and Study 2 (chronic phase after creation of reperfused myocardial infarction). MI, rabbits with reperfused myocardial infarction; MI-VS, MI rabbits treated with vagal nerve stimulation. Three rabbits in Study 1 and 7 rabbits in Study 2 were used as normal controls (not shown in this figure).

change compared with NC values, the means of which were arbitrarily set as 100%.

Enzyme-Linked Immunosorbent Assay. Myocardial tissue sample obtained from the LV lateral wall (infarct and peri-infarct regions in MI and MI-VS rabbits) was homogenized and processed as described previously.

Enzyme-linked immunosorbent assays for C-reactive protein (CRP) (KT-097, Kamiya Biomedical Company, Seattle, WA) and TIMP-1 (RPNJ409, Daiichi fine chemical) were performed using the supernatants of myocardial tissue homogenates from the infarct region according to the manufactures' instructions.[12] Enzyme-linked immunosorbent assays for IL-6 (900-033, Assay Designs, Ann Arbor, MI) was performed using the supernatants of myocardial tissue homogenates from the peri-infarct region. The reason for using the peri-infarct region instead of the infarct region for IL-6 measurement was based on a previous finding that IL-6 mRNA is intensely induced in myocytes of the viable border zone, and not the necrotic infarct zone in myocardial ischemia-reperfusion.[16]

Gelatin Zymography. Tissue sample from the LV lateral wall was homogenized in lysis buffer (50 mM Tris, pH 7.4). The homogenate was centrifuged at 2000g for 10 minutes at 4 °C and the supernatant was collected. Protein concentration of each supernatant sample was determined as described previously.

Gelatin zymography was performed to assess the relative contents of the gelatinases MMP-2 and MMP-9 as described previously.[12] The supernatants (30 μg protein) were loaded in Novex gels containing 0.1% gelatin (Invitrogen, Carlsbad, CA) and then electrophoresed. After renaturation, equilibration, and incubation for 20 hours at 37 °C in developing buffer, the gels were stained in 0.5% Coomassie Blue G-250. Gels were dried and scanned. MMP-2— and MMP-9—related bands were analyzed using the densitometric analysis software.

Determination of Neutrophil Infiltration. The middle ring slice of LV was embedded in paraffin, sectioned at a thickness of 5 μm, and stained with hematoxylin and eosin. We counted the numbers of neutrophils per field in the infarcted area. Neutrophil infiltration into ischemic myocardium was also quantified by evaluating myeloperoxidase activity. Tissue sample from the LV lateral wall was homogenized in potassium phosphate buffer (50 mM, pH 6.4) containing 0.5% hexadecyltrimethylammonium

bromide (WAKO, Japan). The homogenate was centrifuged at 4 °C at 12,000g for 10 minutes and the resultant supernatant was reacted with 0.167 mg/mL of o-dianisidine dihydrochloride (Sigma-Aldrich, St. Louis, MO) and 0.0005% H_2O_2 in potassium phosphate buffer. The change in absorbance at 450 nm was measured spectrophotometrically over 2 minutes. One unit of myeloperoxidase activity was defined as that quantity of enzyme that hydrolyzed 1 μM of peroxide per minute at 25 °C.

Study 2: Chronic Phase after MI

Study 2 consisted of 3 groups of rabbits: MI (n = 16), MI-VS (n = 14), and NC (n = 7).

Echocardiography. Echocardiography was performed under conscious condition at baseline and at 3 days and 8 weeks after coronary reperfusion. Two-dimensional, targeted M-mode tracings were obtained at the level of the papillary muscles with an echocardiographic system equipped with a 7-MHz transducer (Power Vision, TOSHIBA, Japan). LV dimensions were measured according to the American Society for Echocardiography leading-edge method for at least 3 consecutive cardiac cycles. Fractional shortening was calculated as (LVEDD-LVESD)/LVEDD×100, where LVEDD is LV end-diastolic diameter and LVESD is LV end-systolic diameter.

Hemodynamic and Plasma MMPs Measurements. Hemodynamic measurements were performed at 8 weeks after reperfusion. Under general anesthesia (sodium pentobarbital, 35 mg/kg^{-1}) and mechanical ventilation with room air, a 3F micromanometer-tipped catheter (Millar Instruments, Houston, TX) was inserted into the right carotid artery for measurement of mean arterial pressure. Next, the catheter was advanced into the LV for measurement of LV pressure. After completing these measurements, blood was sampled from the right carotid artery. The animal was euthanized. The whole heart was quickly excised and washed with cold phosphate-buffered saline.

Relative protein contents of MMP-2 and MMP-9 in plasma were measured with use of the gelatin zymography as described previously.

LV Passive Pressure-volume Relationship. The excised heart was perfused with a cold, hypocalcemic, hyperkalemic cardioplegic solution (NaCl: 130 mM, KCl: 20 mM, $CaCl_2$: 0.08

mM, lidocaine: 0.5 μg/mL; pH 7.3; 310 mOsm). The passive LV pressure-volume relationship of the arrested heart was measured as described previously.[17] In brief, a compliant water-filled latex balloon tied on a rigid Y-connector was placed in the left ventricle and secured at the mitral annulus with a purse-string suture. Pressure within each balloon was measured with a catheter-tipped micromanometer (Millar Instruments) as volume was progressively increased. Pressure was then plotted as a function of volume at each step, resulting in a passive pressure-volume relationship equivalent to the end-diastolic pressure-volume relationship of the beating heart.[17] The size of the left ventricle was indexed by the volume at which LV pressure reached 10 mm Hg (LVV_{10}).

Infarct Characterization. The coronary branch was reoccluded and 5 mL 0.25% Evans blue was injected from the aorta at 80 mm Hg. After the vasculature, right ventricular free wall, and atrial appendages were dissected, the left ventricle was weighed and fixed in 4% paraformaldehyde overnight. The left ventricle below the coronary artery ligation site was cut into ~5 transverse slices parallel to the atrioventricular ring. Each slice was photographed. The risk area unstained by the blue dye and the non-risk area stained by the blue dye were demarcated. For each slice, the risk area size was determined as the total circumference of the risk area divided by total LV circumference (in percent). The risk area sizes of all slices were averaged and expressed as the risk area size for each heart. The fixed slices from the apex, middle ring, and base were then embedded in paraffin and sectioned at a thickness of 5 μm.

The 5-μm thick cross-sections of left ventricle were stained with Masson's trichrome and Sirius red. Using sections stained with Masson's trichrome, infarct size was determined as the total infarct circumference divided by total LV circumference (in percent). The thicknesses of septal (non-infarct area) and LV lateral walls (infarct area) were measured. The thinning ratio, an index of the extent of wall thinning in the infract, is calculated by dividing the infarct wall thickness by septal wall thickness. Cardiomyocyte cross-sectional areas were determined in the non-infarcted septal myocardium. Only cardiomyocytes cut in cross section were measured. Using sections stained with Sirius red, collagen densities in noninfarcted regions were determined as described previously.[18] Histological images were obtained with a microscope system (BZ 9000, Keyence, Japan), and analyzed using the National Institutes of Health Image software (Image J 1.37). The infarct sizes of the 3 sections (apex, middle ring, base) were averaged and expressed as the LV infarct size for each heart. The thickness of LV wall, cardiomyocyte cross-sectional area, and collagen density were determined in the section that most clearly transverses the infarct region.

Statistical Analyses

All data are presented as mean ± SEM values. Mortalities in the MI and MI-VS groups were compared using chi-square test. Between-group comparison of means obtained at a single time point was performed by Student's unpaired t-test or 1-way analysis of variance. Between-group comparisons of the changes of means over time were conducted using two-way repeated measure analysis of variance to examine any group-time effect. All analyses of variance showing significant differences were further analyzed by post hoc comparison using Student-Newman-Keuls test (Statistica, Statsoft, Inc., Tulsa, OK). P values less than .05 were considered statistically significant.

Results

Study 1: Acute Phase after MI

Body Weight and Mortality. Baseline body weight were comparable among the NC (2490 ± 38 g), MI (2656 ± 64 g), and MI-VS (2517 ± 31 g) groups. Two MI and 2 MI-VS rabbits died from arrhythmia at MI induction. There was no difference in mortality rate up to 24 hours after coronary reperfusion between the MI and MI-VS groups (25% vs. 25 %, P = NS).

HR. Changes of HR over time are summarized in Table 1. There were no significant differences in HR between the MI and MI-VS groups at baseline, after 30 minutes of coronary occlusion, and at 24 hours after coronary reperfusion. No significant time effects on HR were observed.

Myocardial Expression of Cytokines, MMPs, and CRP. Figure 2A shows representative Western blots for TNF-α in the infarcted myocardium. Densitometric analysis demonstrated that TNF-α protein level increased significantly in the MI and MI-VS groups compared with NC value, whereas TNF-α level in the MI-VS group was significantly lower than that in the MI group (<50%, $P < .05$, Fig. 2A). Myocardial protein expressions of IL-1β and IL-6 are summarized in Table 2. There were no significant differences in IL-1β level among the 3 groups. Myocardial levels of IL-6 increased significantly to similar degrees in the MI and MI-VS groups compared with NC values.

As shown in Fig. 2B, zymography of the myocardial extracts detected 2 bands at 92 kDa and 72 kDa corresponding to pro-MMP-9 and pro-MMP-2, respectively. In 2 of 11 MI hearts, but in none of 10 MI-VS hearts, a faint gelatinolytic band was also observed at 83 kDa, which presumably represents the active form of MMP-9.[19] To evaluate the relative content of MMP-9, we used the 92 kDa band (pro-MMP-9) because this band is representative of the global MMP-9 activity.[20] Relative MMP-9 level increased significantly in the MI and MI-VS groups compared with NC value. Level of MMP-9 in the MI-VS group was significantly lower than that in the MI group (<40%, $P < .05$, Fig. 2B). There were no significant differences in MMP-2 (pro-MMP-2) protein level among the 3 groups. Western

Table 1. Changes of Heart Rate with Time after Myocardial Ischemia-reperfusion (Studies 1 and 2)

	Baseline	30 Minutes	24 Hours	3 Days
Study 1				
MI	(n = 6)	277 ± 8	244 ± 24	257 ± 12
MI-VS	(n = 6)	256 ± 8	243 ± 6	250 ± 7
Study 2				
MI	(n = 11)	268 ± 10	245 ± 10	309 ± 11*,†
MI-VS	(n = 10)	264 ± 22	224 ± 11	313 ± 15†

MI, myocardial infarction; MI-VS, myocardial infarction treated with vagal nerve stimulation; 30 minutes, 30 minutes after coronary occlusion; 24 hours, 24 hours after coronary reperfusion; 3 days, 3 days after coronary reperfusion.

Heart rate data (beat/min) are means ± SEM.

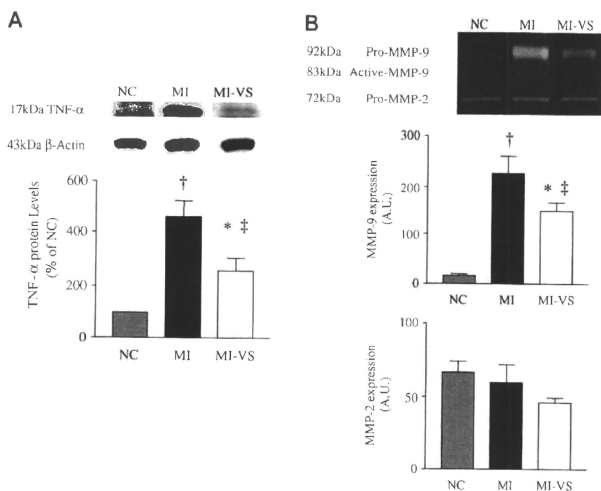*$P < .05$ versus baseline.

†$P < .01$ versus 30 minutes.

Fig. 2. Myocardial protein expressions of tumor necrosis factor-α (TNF-α) and matrix metalloproteinases (MMPs) in normal control rabbits (NC, n = 3), rabbits with reperfused myocardial infarction (MI) (n = 6), and MI rabbits treated with vagal nerve stimulation (MI-VS) rabbits (n = 6). (A) Representative Western blots of TNF-α (17 kDa) as well as corresponding β-actin bands (43 kDa) and band intensities normalized to NC values are shown. (B) Representative zymogram shows pro-MMP-9 band at 92 kDa and pro-MMP-2 band at 72 kDa. Note the faint 83 kDa band in MI hearts, which represents active MMP-9. Densitometric analysis of MMP-9 and MMP-2 contents expressed in integrated optical density (A.U.) relative to background. Data are means ± SEM. *P < .05, †P < .01 versus NC. ‡P < .05 versus MI.

blot analysis of other species of MMPs is summarized in Table 2. Myocardial protein levels of MMP-1 (50 kDa, pro-MMP-1) and MMP-7 (28 kDa, pro-MMP-7) decreased significantly in the MI and MI-VS groups compared to NC values. Myocardial protein level of MMP-8 (75 kDa, pro-MMP-8) increased significantly in the MI group compared with NC and MI-VS values (Table 2).

Table 2. Myocardial Protein Expression (Study 1)

	NC (n)	MI (n)	MI-VS (n)
IL-1β, % of NC	100 ± 6 (3)	79 ± 8 (6)	105 ± 25 (5)
IL-6, ng/g protein	52 ± 2 (3)	100 ± 7 (3) *	97 ± 13 (4)*
MMP-1, % of NC	100 ± 6 (3)	54 ± 8 (6) †	71 ± 12 (6)*
MMP-7, % of NC	100 ± 18 (3)	40 ± 10 (3) *	18 ± 2 (3)†
MMP-8, % of NC	100 ± 15 (3)	510 ± 82 (3) †	236 ± 65 (3)‡
TIMP-1, ng/g protein	39 ± 1 (3)	1394 ± 101 (6)†	1387 ± 164 (6)†
CRP, μg/g protein	13 ± 3 (3)	1926 ± 225 (6)†	1741 ± 114 (6)†

IL, interleukin; MMP, matrix metalloproteinase; TIMP, tissue inhibitor of metalloproteinase; CRP, C-reactive protein.
Data are means ± SEM. The number of hearts used for each experiment is given in parentheses.
*P < .05.
†P < .01 versus NC.
‡P < .05 versus MI.

Myocardial level of TIMP-1 protein increased significantly to similar degrees in MI and MI-VS groups compared with NC values (Table 2).

Myocardial level of CRP increased significantly to similar degrees in the MI and MI-VS groups compared with NC values (Table 2).

Neutrophil Infiltration. No myocardial neutrophil infiltration was found in NC rabbits, whereas intense neutrophil infiltration into the infarcted myocardium was observed in MI rabbits (Fig. 3A). On the other hand, a significantly reduced neutrophil density in the infarcted myocardium was evident in MI-VS rabbits compared with MI animals (Fig. 3A, B). In accordance with neutrophil counts, myeloperoxidase activity in MI-VS rabbits was significantly reduced compared with MI animals (Fig. 3C).

Study 2: Chronic Phase after MI

Body Weight and Survival. Baseline body weights were comparable among the NC (2693 ± 184 g), MI (2530 ± 38 g), and MI-VS (2462 ± 24 g) groups. At 3 days after coronary reperfusion, body weights decreased to the same extent in both the MI (2325 ± 38 g) and MI-VS (2361 ± 53 g) groups. At 8 weeks after reperfusion, body weights increased to similar degrees in the MI (2843 ± 69 g) and
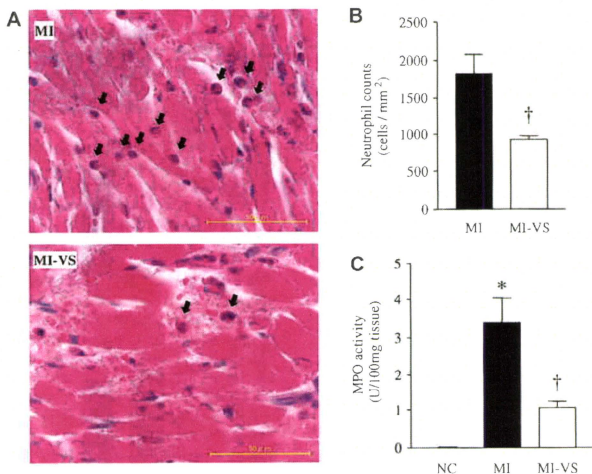
Fig. 3. (A) Photomicrographs of hematoxylin-eosin stained left ventricle cross-sections in infarcted regions obtained from rabbits with re-perfused myocardial infarction (MI) and MI rabbits treated with vagal nerve stimulation (MI-VS) rabbits at 24 hours after coronary reper-fusion. Arrows indicate infiltrating neutrophils. Bars = 50 μm. (B) Neutrophil counts of sections in infarct regions from MI (n = 6) and MI-VS (n = 6) rabbits. (C) Myocardial myeloperoxidase (MPO) activity in NC rabbits (n = 3), and in the infarct regions from MI (n = 4) and MI-VS (n = 4) rabbits. *P < .01 versus NC, †P < 0.01 versus MI.

MI-VS (2899 ± 53 g) groups compared with the respective baseline values.

Five MI and four MI-VS rabbits died and the mortality rate up to 8 weeks after coronary reperfusion was compara-ble between the MI and MI-VS groups (31% versus 29%, P = NS). Of these deaths, 2 MI (13%) and 3 MI-VS (21%) rabbits died from arrhythmia at MI induction (P = NS).
Hemodynamics and LV Function. HR at 3 days after coronary reperfusion significantly increased in both the MI and MI-VS groups from their respective baseline values (Table 1). There were no significant differences in HR be-tween the MI and MI-VS groups at baseline, after 30 min-utes of coronary occlusion, and at 3 days after coronary reperfusion.

Baseline LV diameters and fractional shortening were similar in the MI and MI-VS groups (Table 3). At 3 days after coronary reperfusion, LV fractional shortening was re-duced and LVESD was increased from baseline in both the MI and MI-VS groups to similar degrees. However, further deterioration of LV fractional shortening at 8 weeks after reperfusion observed in MI rabbits was prevented in MI-VS rabbits (Table 3). At 8 weeks after coronary reperfusion, MI-VS rabbits showed significantly smaller LVESD and LVEDD compared with MI rabbits. Data of invasive hemo-dynamic study are summarized in Table 4. Because 2 rab-bits in the MI group with severely depressed LV function (LVEDD > 20 mm, LV fractional shortening < 14%) de-veloped cardiac arrest during the induction of anesthesia,

they were excluded from the invasive hemodynamic study. LV end-diastolic pressure was significantly increased in MI rabbits, which was significantly attenuated in MI-VS rabbits.
LV Passive Pressure-volume Relationship and LV Weight. Plots of ex vivo LV passive pressure-volume re-lationship are shown in Fig. 4A. A marked difference

Table 3. Changes in Echocardiographic Parameters with Time (Study 2)

	Baseline	3 Days	8 Weeks
LVESD, mm			
MI	7.8 ± 0.2	10.9 ± 0.2[1]	15.5 ± 0.6[1,§]
MI-VS	7.9 ± 0.4	9.8 ± 0.5*	11.4 ± 1.1[1,#]
LVEDD, mm			
MI	13.0 ± 0.3	14.6 ± 0.3	19.2 ± 0.6[1,§]
MI-VS	12.8 ± 0.3	13.3 ± 0.5	15.5 ± 1.0[1,‡,#]
FS, %			
MI	39.9 ± 1.3	24.9 ± 1.5[†]	19.6 ± 1.6[1,‡]
MI-VS	38.6 ± 1.9	27.1 ± 1.2[†]	27.2 ± 2.6[1,‖]

3 d, 3 days after coronary reperfusion; 8 w, 8 weeks after coronary re-perfusion; LVESD, left ventricular (LV) end-systolic diameter; LVEDD, LV end-diastolic diameter; FS, LV fractional shortening.
Data are means ± SEM.
n = 11 in MI group.
n = 10 in MI-VS group.
*P < .05.
[1]P < .01 versus baseline.
[‡]P < .05.
[§]P < .01 versus 3 days.
[‖]P < .05.
[#]P < .01 versus MI.

Table 4. Invasive Hemodynamic Parameters 8 Weeks after Coronary Reperfusion (Study 2)

	NC	MI	MI-VS
HR, beat/min	335 ± 14	320 ± 5	322 ± 5
MAP, mm Hg	110 ± 3	112 ± 3	112 ± 4
LV dP/dt$_{max}$, mm Hg/s	4622 ± 234	4546 ± 229	4770 ± 348
LV EDP, mm Hg	4 ± 1	16 ± 3*	7 ± 2†

NC, normal control; HR, heart rate; MAP, mean arterial pressure; LV dP/dt$_{max}$, the maximum first derivative of left ventricular pressure; LV EDP, left ventricular end-diastolic pressure.

Data are means ± SEM.

n = 7 in NC group, n = 9 in MI group, n = 10 in MI-VS group.

*P < .01 versus NC.

$^†P$ < .05 versus MI.

between NC and MI hearts is evident, whereas the average curve derived from MI-VS hearts is close to that of NC hearts. As shown in Fig. 4B, LV size, indexed by LVV$_{10}$, of MI-VS hearts was significantly smaller than that of MI hearts (P < .01) and reached values close to those of NC hearts. LV weight normalized by body weight increased significantly in both MI and MI-VS hearts compared with NC value (Fig. 4C), but was significantly lower in MI-VS hearts than in MI hearts (P < .01).

Histomorphologic Analysis of LV. The risk area sizes were comparable in MI and MI-VS hearts (47 ± 3% vs. 51 ± 5%, P = NS). A transverse LV section demonstrated

a smaller LV cavity in the heart receiving VS (Fig. 5A). The LV infarct size was significantly reduced in MI-VS hearts (P < .05) compared with MI hearts as shown in Fig. 5B. Because the risk area sizes were comparable in MI and MI-VS hearts, the reduction of infarct size seen in MI-VS rabbits was due to the VS treatment, not insufficient ischemic insults. Wall thickness in LV septum (non-infarct region) was comparable in MI and MI-VS hearts, whereas LV infarct wall thickness was significantly greater in MI-VS hearts than in MI hearts. This resulted in higher thinning ratios in MI-VS hearts than in MI hearts (Fig. 5B). Myocyte hypertrophy in the septum was attenuated in MI-VS hearts as demonstrated by significantly reduced myocyte cross-sectional area compared with MI hearts. Collagen densities in viable myocardial tissue were similar in MI and MI-VS hearts (11 ± 1% versus 9 ± 0%, P = NS).

Plasma MMP. Relative MMP-9 level in plasma was comparable among NC (156 ± 19 A.U., n = 6), MI (147 ± 28 A.U., n = 7), and MI-VS (146 ± 22 A.U., n = 7) groups. Relative MMP-2 level in the MI-VS group (164 ± 20 A.U.) was significantly lower compared with those in the NC (226 ± 17 A.U.) and MI (230 ± 16 A.U.) groups (P < .05).

Subgroup Analysis of Effects of VS on LV Remodeling in Large MI. Because the progression of LV remodeling is problematic, especially in patients with large infarct
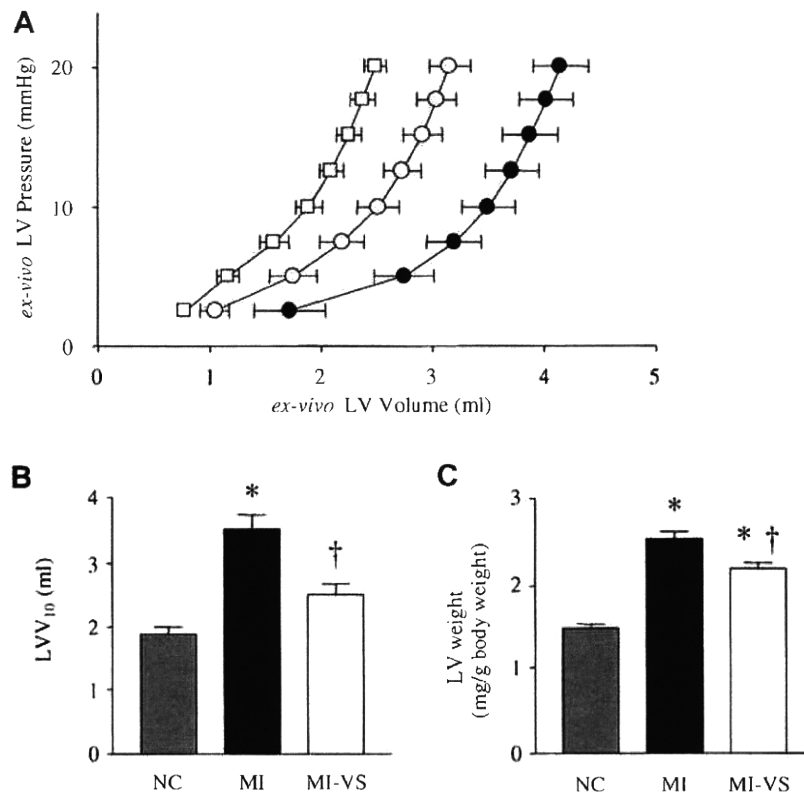

Fig. 4. Ex vivo left ventricular (LV) examinations of normal control (NC) (n = 7), reperfused myocardial infarction (MI) (n = 11), and MI rabbits treated with vagal nerve stimulation (MI-VS) (n = 10) hearts. (A) LV passive pressure-volume relationship in NC (□), MI (●), and MI-VS (○) hearts. (B) Ex vivo LV volume at LV pressure of 10 mm Hg (LVV$_{10}$). (C) LV weight normalized by body weight. *P < .01 versus NC. $^†P$ < .01 versus MI.
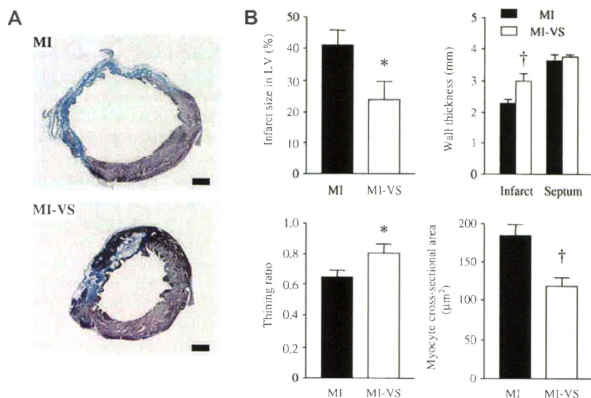
Fig. 5. (A) Transverse LV sections obtained from reperfused myocardial infarction (MI) and MI rabbits treated with vagal nerve stimulation (MI-VS) hearts 8 weeks post-MI. The sections were stained with Masson's trichrome. Blue stained area indicates scared infarct area. Bars = 3 mm. (B) Histomorphometric analyses of LVs in MI (n = 11) and MI-VS (n = 10) hearts. *P < .05, †P < .01 versus MI.

size,[1] we evaluated the effects of VS on the parameters of LV remodeling (LV weight and LVEDD at 8 weeks after coronary reperfusion) in animals with large infarct size (>30% of LV, 8 MI. and 4 MI-VS rabbits). LV infarct size was comparable in MI and MI-VS hearts (49 ± 3% versus 44 ± 6%, P = NS). However, LV weight was significantly lower in MI-VS hearts than in MI hearts (2.2 ± 0.1 versus 2.6 ± 0.1 mg/g body weight, P < .05). There was a strong trend of reduction in LVEDD in MI-VS hearts compared with MI hearts, although the difference did not reach statistical significance (15.1 ± 2.0 versus 18.9 ± 0.8 mm, P = .052).

Discussion

The major new findings of the present study were as follows. In the acute inflammatory phase of reperfused MI, VS decreased TNF-α protein level and suppressed neutrophil infiltration in the infarcted myocardium. In the chronic phase of reperfused MI, VS markedly attenuated LV dysfunction and remodeling, even though VS was limited to a short period early after MI. Although several acute experimental studies examined the cardioprotective effects of VS in reperfused MI, they lacked detailed assessment of LV function and structure as done in this study.[5–7]

Cardioprotective Effects of VS and Cytokine Expressions

The beneficial effects of VS on reperfused MI are primarily attributable to the reduction of infarct size.[1,21] Several cardioprotective mechanisms of VS in ischemic myocardium have been reported previously. In a

neutrophil-free isolated heart preparation, VS attenuated ischemia-reperfusion injury by protecting the myocytic mitochondria.[5] In a non-reperfused MI model, VS protected cardiomyocytes by upregulating hypoxia-inducible factor-1α pathway, and reduced infarct size.[22] Acetylcholine, the principal vagal neurotransmitter, mediated these direct protective effects on cardiomyocyte through the muscarinic acetylcholine receptor pathway.[5,22] These mechanisms may have contributed to the reduction of infarct size by VS in the present study. In addition, suppression of myocardial neutrophil infiltration in acute MI phase might also contribute to the reduction of infarct size by VS. Although reperfusion of the ischemic myocardium is necessary to salvage viable myocytes from eventual death, reperfusion also causes tissue damage.[9] Reperfusion injury in the acute phase of MI shares many characteristics with inflammatory reactions. Neutrophils feature prominently in this inflammatory reaction.[9] It is well known that in the reperfused ischemic myocardium, upregulated TNF-α accelerates the infiltration of neutrophils.[8,23] In this study, VS suppressed neutrophil infiltration into the infarcted myocardium possibly through inhibition of TNF-α expression, which might suppress the neutrophil-induced myocyte injury, thereby reducing the infarct size. Acetylcholine attenuates the release of TNF-α from macrophages through the nicotinic acetylcholine receptor pathway.[10,11] Cardiac mast cell is an important source of TNF-α in ischemic myocardium,[23] and expresses the nicotinic receptor.[24] In our model, VS might have directly reduced TNF-α expression on cardiac mast cells via the nicotinic acetylcholine receptor pathway.

Myocardial IL-1β protein content was not changed in our MI model. Previous experimental study also reported

similar results and suggested an insignificant role of IL-1β as an upstream inducer of post-reperfusion inflammatory reactions.[23] Myocardial IL-6 protein expression was not affected by VS in this study. Previous clinical study indicated that VS decreased plasma IL-6 concentration in patients with advanced heart failure, but the reduction was transient and noted only at 3 months after commencing VS.[4] Although the increase in plasma IL-6 has been associated with progression of LV contractile dysfunction in patients with heart failure, recent experimental research suggests that IL-6 expression in viable myocardium may play a pivotal role in cytoprotection.[25] Several biochemical and hemodynamic factors have been shown to regulate IL-6 expression after MI. IL-6 mRNA expression in mononuclear cells infiltrating the infarcted myocardium is upregulated by TNF-α.[23] Gwechenberger et al[16] have shown the reperfusion-dependent expression of IL-6 mRNA in cardiomyocytes in the viable border zone. Perfusion dependency of IL-6 expression was also observed in patients with reperfused MI, where plasma IL-6 concentration positively correlated with ischemic myocardial collateral flow.[26] In the present study, VS-induced TNF-α reduction might have decreased myocardial IL-6 expression. On the other hand, the beneficial effect of VS on myocardial perfusion[27] or the direct cardiomyocyte-protecting effect of VS[5] might have increased de novo synthesis of IL-6 in the jeopardized but viable myocardium. In VS, all these factors may operate simultaneously.

Myocardial CRP expression increased drastically after MI, which was not affected by VS in this study. After MI, CRP is produced from the liver partly as a response to stimulation by IL-6 released from the damaged heart.[28] Because we found that cardiac expression of IL-6 was similar in the MI and MI-VS groups, it is reasonable that myocardial CRP content was not different between the 2 groups in the present experiment. CRP-mediated complement activation in the myocardium was associated with increase in infarct size and LV remodeling after MI in several experimental and clinical studies,[28,29] although this association remains controversial.[30,31]

Our previous studies suggest that bradycardia plays a significant role in cardioprotection by VS.[3] However, the present results indicate that the cardioprotective effect of VS does not necessarily require strong bradycardia. Huston et al demonstrated that in a mouse model of sepsis, mild intensity of VS drastically reduces serum TNF-α without inducing bradycardia.[11] Furthermore, the cardioprotective effect of VS through protecting myocytic mitochondria is also independent of the degree of bradycardia.[5] Increasing VS intensity to attain strong bradycardia can cause unwanted side effects such as local pain in animals and also in patients.[3,4] Although the degree of bradycardia has been the primary parameter used in adjusting the intensity of VS,[4] additional parameters may be required for deciding the proper therapeutic strategy of VS in clinical application.

MMP Inhibition and LV Remodeling. Subgroup analysis of study 2 demonstrated that VS attenuated LV hypertrophy when comparing MI and MI-VS hearts with similarly large infarct size. This finding indicates that VS indeed confers an antiremodeling effect beyond that through reduction in infarct size. Reduction of MMP-9 activity in the infarcted myocardium early after MI may contribute to this antiremodeling effect of VS.[18,32–34] In addition to the loss of contractile cardiomyocytes, pathological degradation and reconstitution of extracellular matrix contribute to the progression of LV remodeling after MI, where MMP and TIMP play crucial roles. After MI, pharmacological MMP inhibition attenuated LV remodeling without affecting infarct size even if given for a short period.[18,33] Suppression of the infiltration of neutrophil, an important source of MMP-9 after myocardial ischemia reperfusion,[32] may be one reason of the reduction of MMP-9 contents by VS in infarct observed in this study. VS did not change the collagen content of the viable myocardium at 8 weeks after MI in spite of reduced MMP-9 expression early after MI. Several studies also reported that MMP inhibition improved LV remodeling without changing the collagen contents within the infarcts or in viable tissues after MI.[18,33] Lindsey et al demonstrated in a rabbit model of MI that inhibition of MMP activities attenuated LV dilatation and preserved the infarct wall thickness and the thinning ratio without changing the tissue collagen content.[33] Their findings are almost compatible to the present results. These observations suggest that a noncollagenolytic mechanism may also play a critical role in regulating LV remodeling. Plasma MMP-9 concentration measured 8 weeks after MI was not reduced in MI-VS rabbits compared with MI rabbits and controls. This indicates that the MMP-9 suppressive effect of VS delivered early after MI did not last long. This might be beneficial in terms of LV remodeling. A previous experimental study[34] demonstrated that MMP inhibition early after MI conferred beneficial effects on LV remodeling, but chronic prolonged MMP inhibition was associated with adverse effects on LV remodeling. MMP-8, a neutrophil collagenase, has been shown to increase in cardiac tissue after MI and relate to LV rupture in MI patients.[35] In this study, suppression of neutrophil infiltration is probably the primary reason for the reduction of myocardial MMP-8 contents by VS.

MMP-1 is mainly produced by cardiac fibroblasts. MMP-2 is mainly expressed in cardiomyocytes after ischemic injury.[35] MMP-7 is expressed in macrophages and cardiomyocytes after MI.[36] After reperfused MI, myocardial protein contents of MMP-1, -2, and -7 were not affected by VS. Taken together, VS appears to specifically affect neutrophil-associated MMPs.

Myocardial TIMP-1 protein level was not affected by VS in this study, which seems inconsistent with our previous finding.[12] TIMP-1 level increased drastically after 24 hours of coronary reperfusion in the present study (> 1200 ng/g protein, compared with that observed after 3 hours of reperfusion in rabbits in our previous study (< 500 ng/g protein).[12] On the other hand, the intensity of VS in this study was rather mild compared with that in the previous

study. These factors together may have obscured the TIMP-1—inducing property of VS in this study.

Clinical Implication

Early short-term VS strategy appears to be clinically feasible in patients with acute MI. Furthermore, this strategy may be both timely and sufficient based on the following evidence. First, upregulation of plasma and myocardial TNF-α as well as myocardial infiltration of neutrophils are mostly confined to within 3 days after MI.[15,37] Meanwhile, the anti-inflammatory effects of VS are long-lasting. In mice, only 30 seconds of VS significantly suppressed TNF-α activation in response to lipopolysaccharide challenge even at 48 hours after VS.[11] Second, pharmacological inhibition of MMP activity for 48 hours after MI preserves the original extracellular matrix, thereby lessens LV remodeling.[18]

Although the present findings suggest clinically useful strategy of VS, several issues remain to be solved before VS can be considered for clinical application in patients with MI. First, it is unclear whether VS is able to provide additional therapeutic benefits to current pharmacological treatments such as renin-angiotensin-aldosterone inhibition or β-blockade, the efficacy of which has been well established in patients with MI.[38] Second, it is unclear whether VS started after reperfusion is also capable of attenuating LV remodeling after MI. Although we started VS during coronary occlusion in this study, initiating VS after coronary reperfusion may simulate a more clinically relevant situation, because prompt reperfusion of occluded coronary artery is given the utmost priority in the management of patients with acute MI. Further studies to solve these problems are clearly required.

VS did not afford any survival benefit in this study, which is inconsistent with previous findings that VS improves acute[7] or chronic[3] survival in rats after MI by preventing malignant arrhythmia and heart failure. However, the mortality rate in MI rats was $\sim 60\%$ within the first 24 hours in the previous study,[3] which is undoubtedly higher than that seen in MI rabbits of this study ($\sim 30\%$). Low mortality rate in MI rabbits may have masked the impact of VS on survival in this study.

Limitation

We focused on the antiremodeling effects of VS but did not include a detailed mechanistic investigation into how VS reduces LV infarct size. Inflammatory responses to MI play a significant role in determining the infarct size.[9] On the other hand, the infarct size, which reflects the degree of myocardial necrosis, is also one of the determinants of post-MI inflammatory reactions. Therefore, direct cardiomyocyte protection of VS possibly through the muscarinic acetylcholine pathway and the anti-inflammatory effect possibly through the nicotinic pathway may have contributed synergistically to the infarct size-reducing effect of VS. Selective inhibition of the muscarinic and nicotinic

pathway by atropine and methyllycaconitine,[39] respectively, may allow elucidation of how these different mechanisms contribute to the beneficial effects of VS in a reperfused MI model. Further studies on these issues are clearly required.

Acute surgical trauma associated with open-chest preparation may have exaggerated the expression of CRP and TNF-α in MI and MI-VS rabbits in this study. For a more rational comparison of acute inflammatory reactions among NC, MI, and MI-VS animals, use of sham-operated rabbits as NC would be more appropriate. Closed-chest animal models of myocardial ischemia-reperfusion[40] may be an alternative to eliminate acute surgical trauma and allow assessment of inflammation strictly from myocardial injury. In this study, MI and MI-VS rabbits underwent identical surgical preparation. Therefore, it is fair to say that the difference in TNF-α expression in infarcts between the MI and MI-VS groups was valid in the present study.

In conclusion, early short-term VS attenuated cardiac dysfunction and myocardial structural remodeling in a rabbit model of reperfused MI. The beneficial effects of VS were associated with suppression of excessive TNF-α activation and myocardial infiltrations of neutrophils.

References

1. Bolognese L, Cerisano G. Early predictors of left ventricular remodeling after acute myocardial infarction. Am Heart J 1999;138:S79—83.
2. Ezekowitz JA, Kaul P, Bakal JA, Armstrong PW, Welsh RC, McAlister FA. Declining in-hospital mortality and increasing heart failure incidence in elderly patients with first myocardial infarction. J Am Coll Cardiol 2009;53:13—20.
3. Li M, Zheng C, Sato T, Kawada T, Sugimachi M, Sunagawa K. Vagal nerve stimulation markedly improves long-term survival after chronic heart failure in rats. Circulation 2004;109:120—4.
4. Schwartz PJ, De Ferrari GM, Sanzo A, Landolina M, Rordorf R, Raineri C, et al. Long term vagal stimulation in patients with advanced heart failure: first experience in man. Eur J Heart Fail 2008;10:884—91.
5. Katare RG, Ando M, Kakinuma Y, Arikawa M, Handa T, Yamasaki F, et al. Vagal nerve stimulation prevents reperfusion injury through inhibition of opening of mitochondrial permeability transition pore independent of the bradycardiac effect. J Thorac Cardiovasc Surg 2009;137:223—31.

6. Kawada T, Yamazaki T, Akiyama T, Kitagawa H, Shimizu S, Mizuno M, et al. Vagal stimulation suppresses ischemia-induced myocardial interstitial myoglobin release. Life Sci 2008;83:490—5.

7. Mioni C, Bazzani C, Giuliani D, Altavilla D, Leone S, Ferrari A, et al. Activation of an efferent cholinergic pathway produces strong protection against myocardial ischemia/reperfusion injury in rats. Crit Care Med 2005;33:2621—8.

8. Sun M, Dawood F, Wen WH, Chen M, Dixon I, Kirshenbaum LA, et al. Excessive tumor necrosis factor activation after infarction contributes to susceptibility of myocardial rupture and left ventricular dysfunction. Circulation 2004;110:3221—8.

9. Vinten-Johansen J. Involvement of neutrophils in the pathogenesis of lethal myocardial reperfusion injury. Cardiovasc Res 2004;61: 481—97.

10. Borovikova LV, Ivanova S, Zhang M, Yang H, Botchkina GI, Watkins LR, et al. Vagus nerve stimulation attenuates the systemic inflammatory response to endotoxin. Nature 2000;405:458—62.

11. Huston JM, Gallowitsch-Puerta M, Ochani M, Ochani K, Yuan R, Rosas-Ballina M, et al. Transcutaneous vagus nerve stimulation reduces serum high mobility group box 1 levels and improves survival in murine sepsis. Crit Care Med 2007;35:2762—8.

12. Uemura K, Li M, Tsutsumi T, Yamazaki T, Kawada T, Kamiya A, et al. Efferent vagal nerve stimulation induces tissue inhibitor of metalloproteinase-1 in myocardial ischemia-reperfusion injury in rabbit. Am J Physiol Heart Circ Physiol 2007;293:H2254—61.

13. LaCroix C, Freeling J, Giles A, Wess J, Li YF. Deficiency of M2 muscarinic acetylcholine receptors increases susceptibility of ventricular function to chronic adrenergic stress. Am J Physiol Heart Circ Physiol 2008;294:H810—20.

14. Hasdemir C, Scherlag BJ, Yamanashi WS, Lazzara R, Jackman WM. Endovascular stimulation of autonomic neural elements in the superior vena cava using a flexible loop catheter. Jpn Heart J 2003;44: 417—27.

15. Dewald O, Ren G, Duerr GD, Zoerlein M, Klemm C, Gersch C, et al. Of mice and dogs: species-specific differences in the inflammatory response following myocardial infarction. Am J Pathol 2004;164:665—77.

16. Gwechenberger M, Mendoza LH, Youker KA, Frangogiannis NG, Smith CW, Michael LH, et al. Cardiac myocytes produce interleukin-6 in culture and in viable border zone of reperfused infarctions. Circulation 1999;99:546—51.

17. Klotz S, Foronjy RF, Dickstein ML, Gu A, Garrelds IM, Danser AH, et al. Mechanical unloading during left ventricular assist device support increases left ventricular collagen cross-linking and myocardial stiffness. Circulation 2005;112:364—74.

18. Villarreal FJ, Griffin M, Omens J, Dillmann W, Nguyen J, Covell J. Early short-term treatment with doxycycline modulates postinfarction left ventricular remodeling. Circulation 2003;108:1487—92.

19. Newman KM, Ogata Y, Malon AM, Irizarry E, Gandhi RH, Nagase H, et al. Identification of matrix metalloproteinases 3 (stromelysin-1) and 9 (gelatinase B) in abdominal aortic aneurysm. Arterioscler Thromb 1994;14:1315—20.

20. Ernens I, Rouy D, Velot E, Devaux Y, Wagner DR. Adenosine inhibits matrix metalloproteinase-9 secretion by neutrophils: implication of A2a receptor and cAMP/PKA/Ca2+ pathway. Circ Res 2006;99: 590—7.

21. Ørn S, Manhenke C, Anand IS, Squire I, Nagel E, Edvardsen T, et al. Effect of left ventricular scar size, location, and transmurality on left ventricular remodeling with healed myocardial infarction. Am J Cardiol 2007;99:1109—14.

22. Kakinuma Y, Ando M, Kuwabara M, Katare RG, Okudela K, Kobayashi M, et al. Acetylcholine from vagal stimulation protects cardiomyocytes against ischemia and hypoxia involving additive non-hypoxic induction of HIF-1alpha. FEBS Lett 2005;579:2111—8.

23. Frangogiannis NG, Lindsey ML, Michael LH, Youker KA, Bressler RB, Mendoza LH, et al. Resident cardiac mast cells degranulate and release preformed TNF-alpha, initiating the cytokine cascade in experimental canine myocardial ischemia/reperfusion. Circulation 1998;98:699—710.

24. Kindt F, Wiegand S, Niemeier V, Kupfer J, Löser C, Nilles M, et al. Reduced expression of nicotinic alpha subunits 3, 7, 9 and 10 in lesional and nonlesional atopic dermatitis skin but enhanced expression of alpha subunits 3 and 5 in mast cells. Br J Dermatol 2008;159: 847—57.

25. Smart N, Mojet MH, Latchman DS, Marber MS, Duchen MR, Heads RJ. IL-6 induces PI 3-kinase and nitric oxide-dependent protection and preserves mitochondrial function in cardiomyocytes. Cardiovasc Res 2006;69:164—77.

26. Rakhit RD, Seiler C, Wustmann K, Zbinden S, Windecker S, Meier B, et al. Tumour necrosis factor-alpha and interleukin-6 release during primary percutaneous coronary intervention for acute myocardial infarction is related to coronary collateral flow. Coron Artery Dis 2005;16:147—52.

27. Buck JD, Warltier DC, Hardman HF, Gross GJ. Effects of sotalol and vagal stimulation on ischemic myocardial blood flow distribution in the canine heart. J Pharmacol Exp Ther 1981;216:347—51.

28. Ørn S, Manhenke C, Ueland T, Damås JK, Mollnes TE, Edvardsen T, et al. C-reactive protein, infarct size, microvascular obstruction, and left-ventricular remodelling following acute myocardial infarction. Eur Heart J 2009;30:1180—6.

29. Nijmeijer R, Lagrand WK, Lubbers YT, Visser CA, Meijer CJ, Niessen HW, et al. C-reactive protein activates complement in infarcted human myocardium. Am J Pathol 2003;163:269—75.

30. Sukhija R, Fahdi I, Garza L, Fink L, Scott M, Aude W, et al. Inflammatory markers, angiographic severity of coronary artery disease, and patient outcome. Am J Cardiol 2007;99:879—84.

31. Blankenberg S, McQueen MJ, Smieja M, Pogue J, Balion C, Lonn E, et al. Comparative impact of multiple biomarkers and N-Terminal probrain natriuretic peptide in the context of conventional risk factors for the prediction of recurrent cardiovascular events in the Heart Outcomes Prevention Evaluation (HOPE) Study. Circulation 2006;114: 201—8.

32. Kelly D, Cockerill G, Ng LL, Thompson M, Khan S, Samani NJ, et al. Plasma matrix metalloproteinase-9 and left ventricular remodelling after acute myocardial infarction in man: a prospective cohort study. Eur Heart J 2007;28:711—8.

33. Lindsey ML, Gannon J, Aikawa M, Schoen FJ, Rabkin E, Lopresti-Morrow L, et al. Selective matrix metalloproteinase inhibition reduces left ventricular remodeling but does not inhibit angiogenesis after myocardial infarction. Circulation 2002;105:753—8.

34. Spinale FG, Escobar GP, Hendrick JW, Clark LL, Camens SS, Mingoia JP, et al. Chronic matrix metalloproteinase inhibition following myocardial infarction in mice: differential effects on short and long-term survival. J Pharmacol Exp Ther 2006;318:966—73.

35. van den Borne SW, Cleutjens JP, Hanemaaijer R, Creemers EF, Smits JF, Daemen MJ, et al. Increased matrix metalloproteinase-8 and -9 activity in patients with infarct rupture after myocardial infarction. Cardiovasc Pathol 2009;18:37—43.

36. Lindsey ML, Escobar GP, Mukherjee R, Goshorn DK, Sheats NJ, Bruce JA, et al. Matrix metalloproteinase-7 affects connexin-43 levels, electrical conduction, and survival after myocardial infarction. Circulation 2006;113:2919—28.

37. Li D, Zhao L, Liu M, Du X, Ding W, Zhang J, et al. Kinetics of tumor necrosis factor alpha in plasma and the cardioprotective effect of a monoclonal antibody to tumor necrosis factor alpha in acute myocardial infarction. Am Heart J 1999;137:1145—52.

38. Landmesser U, Wollert KC, Drexler H. Potential novel pharmacological therapies for myocardial remodelling. Cardiovasc Res 2009;81: 519—27.

39. Liu C, Shen FM, Le YY, Kong Y, Liu X, Cai GJ, Chen AF, Su DF. Antishock effect of anisodamine involves a novel pathway for activating alpha7 nicotinic acetylcholine receptor. Crit Care Med 2009;37: 634—41.

40. Nossuli TO, Lakshminarayanan V, Baumgarten G, Taffet GE, Ballantyne CM, Michael LH, et al. A chronic mouse model of myocardial ischemia-reperfusion: essential in cytokine studies. Am J Physiol Heart Circ Physiol 2000;278:H1049—55.

ORIGINAL PAPER

Both skeletonized and pedicled internal thoracic arteries supply adequate graft flow after coronary artery bypass grafting even during intense sympathoexcitation

Dai Une · Shuji Shimizu · Atsunori Kamiya ·
Toru Kawada · Toshiaki Shishido · Masaru Sugimachi

Abstract The internal thoracic artery (ITA) is harvested by either the pedicled or the skeletonized technique in coronary artery bypass grafting (CABG), with no clear advantage of one technique over the other. We compared graft flow between the pedicled and skeletonized ITA grafts while varying myocardial oxygen demand. CABG was performed to the left anterior descending artery in five anesthetized dogs using a pedicled ITA graft and the graft was subsequently skeletonized. Graft flow was measured during stepwise electrical stimulation of the stellate ganglion. The baseline graft flow before sympathetic stimulation was higher in skeletonized (27.8 ± 1.9 ml/min) than that in pedicled ITA grafts (22.6 ± 2.7 ml/min) ($P < 0.05$). In both ITA grafts, however, graft flow increased to a similar level during sympathetic stimulation that doubled the double product, correlating with the double product. Based on these results, we conclude that metabolic demand can override the potential difference in sympathetic vasoconstriction in both pedicled and skeletonized ITA grafts.

Keywords Coronary artery bypass grafting · Graft flow · Internal thoracic artery · Pedicled · Skeletonized · Sympathetic activation

D. Une · S. Shimizu (✉) · A. Kamiya · T. Kawada ·
T. Shishido · M. Sugimachi
Department of Cardiovascular Dynamics, National Cerebral and Cardiovascular Center Research Institute,
5-7-1 Fujishiro-dai, Suita, Osaka 565-8565, Japan
e-mail: shujismz@ri.ncvc.go.jp

S. Shimizu
Japan Association for the Advancement of Medical Equipment, Tokyo, Japan

Introduction

The internal thoracic artery (ITA) is the gold standard conduit for coronary artery bypass grafting (CABG) because of its long-term patency [1]. The ITA is harvested by either the pedicled or the skeletonized technique, and which of these two techniques is the better option has been the subject of an extended debate—with as yet no clear conclusion being drawn. Although some human studies [2–4] have demonstrated higher free (pre-anastomosis) flow through skeletonized grafts (with or without topical papaverine), suggesting that the loss of sympathetic nerve-mediated graft vasoconstriction confers an advantage, perfusion pressure was not controlled in these studies. In one study [5] in which the perfusion pressure was controlled, free flow even tended to be lower in skeletonized grafts prior to the administration of intravenous papaverine. Onorati et al. [6] found that graft flows were comparable between the two techniques in the absence of intraluminal papaverine, while Takami and Ina [7], in a comparison of the flow through the anastomosed graft, found that flow was higher through the skeletonized graft.

Flow in the anastomosed graft is likely to be largely dependent on myocardial oxygen demand, suggesting the importance of comparing the flow between the pedicled and skeletonized ITA grafts under varying conditions of myocardial oxygen demand. If the skeletonization procedure were to result in an increased flow capacity, surgeons may be able to perform additional anastomoses to other vessels using the skeletonized ITA, thereby making the skeletonized ITA procedure even more advantageous. If the skeletonization procedure were not able to increase flow capacity, the skeletonized ITA would not be recommended for additional use due to a higher flow reserve. We hypothesized that the skeletonized ITA would have larger

flow capacity due to the loss of sympathetic nerve-mediated graft vasoconstriction.

Materials and methods

Animal preparation

Animal care was provided in accordance with the *Guiding Principles for the Care and Use of Animals in the Field of Physiological Sciences* approved by the Physiological Society of Japan. All protocols were approved by the Animal Subject Committee of the National Cerebral and Cardiovascular Center. Five adult mongrel dogs (weighing 24–35 kg) were anesthetized with intravenous pentobarbital sodium (25 mg/kg) and intubated endotracheally for artificial ventilation with isoflurane and 100% O_2. After a median sternotomy, the heart was suspended in a pericardial cradle. To measure systemic arterial pressure, we placed a fluid-filled catheter in the left subclavian artery via the left brachial artery and connected it to a pressure transducer (DX-200; Nihon Kohden, Tokyo, Japan). The junction of the inferior vena cava and the right atrium was taken as the reference point for zero pressure. An ultrasonic flowmeter (20A594; Transonic Systems, Itaca, NY) was placed around the ascending aorta to measure cardiac output. Electrocardiography leads were also placed for the monitoring electrocardiogram. A catheter was inserted into the femoral vein for fluid replacement (1 ml/kg/h of Ringer's solution). All protocols were performed under open chest conditions.

Pedicled ITA grafting

The left internal thoracic artery (LITA), together with the surrounding veins, muscle, and fascia, was harvested as a pedicled graft using electrocautery. The LITA was harvested from the bifurcation of the musculo-phrenic and superior epigastric arteries up to the upper margin of the first rib or higher. All intercostal branches of the LITA were ligated. After systemic heparinization, the LITA was clamped, and the distal end of the LITA was cut and anastomosed to the left anterior descending artery (LAD). The same surgeon (D.U.) performed the LITA–LAD anastomosis without cardiopulmonary bypass. The heart and the LAD were stabilized using a compression-type mechanical stabilizer (Mini-CABG system; United States Surgical Corporation, Norwalk, CT). A shunt tube was inserted into the LAD to prevent myocardial ischemia during anastomosis. The anastomosis was placed in the mid-LAD [8]. The anastomosis was created using a continuous 7-0 polypropylene suture. The proximal LAD was first ligated after the LITA–LAD anastomosis, and then the

LITA was declamped. An angiography was performed after the anastomosis to confirm the absence of stenosis or spasm in the LITA–LAD anastomosis. The LITA graft was sprayed with dilute papaverine (4 mg/ml) to prevent spasm. An ultrasonic flowmeter (2.5S261; Transonic Systems) was placed around the LITA just proximal to the anastomosis. The left stellate ganglion was carefully exposed through a median sternotomy, and a pair of platinum electrodes was attached to it without decentralization. The nerve and electrodes were covered with a mixture of silicone gel (Kwik-Sil; World Precision Instrument, Sarasota, FL). Protocol 1, described below, was carried out following the pedicled LITA grafting.

Skeletonized ITA grafting

Following the completion of protocol 1, the tissue surrounding the graft (including fascia and lymphatics) was stripped up to the most proximal part of the LITA graft in order to skeletonize the LITA graft. The side branches of the LITA were ligated. Fat tissue around the graft was removed as completely as possible based on macroscopic inspection. The adventitia was left as the outermost layer of the graft. The graft was not touched directly with forceps. The graft was sprayed with dilute papaverine (4 mg/ml). After skeletonizing the LITA graft, protocol 2 followed.

Experimental protocols

Since skeletonization always followed pedicled harvesting, protocol 1 (pedicled LITA graft flow measurement) was performed before protocol 2 (skeletonized LITA graft flow measurement) in all dogs. The stimulation of the left sympathetic stellate ganglion for adjusting the voltage amplitude was performed at least 30 min before protocol 1 was initiated.

Protocol 1

The left sympathetic stellate ganglion was electrically stimulated at least 30 min after the completion of the experimental preparation of the pedicled LITA grafts. The frequency of stimulation was increased stepwise from 0 to 10 Hz with increments of 2 Hz. Each step was maintained for 60 s. The pulse duration of the stimulus was set at 5 ms. The voltage amplitude of stimulation (2–5 V) was adjusted in each animal to yield an increase in arterial pressure of approximately 30 mmHg with 10 Hz stimulation. Graft flow, arterial pressure, and cardiac output were recorded for 7 min, which included a 2-min baseline and 5 min of stimulation. These data were sampled at 200 Hz using a 12-bit analog-to-digital converter [AD12-16U(PCI)E;

CONTEC, Osaka, Japan] and stored on the hard disk of a dedicated laboratory computer system.

Protocol 2

At least 30 min after the completion of the experimental preparation of the skeletonized LITA grafts, the left sympathetic stellate ganglion was electrically stimulated in a similar fashion to protocol 1, while all variables were recorded and stored.

Data analysis

Heart rate was calculated from the arterial pressure waveform. Myocardial oxygen demand was estimated as double product (pressure–rate product) and calculated as the product of systolic arterial pressure and heart rate [9]. All variables were averaged during the last 20 s of each electrical stimulation level.

Statistical analysis

All data are presented as the mean $\pm$ standard error (SE). In each protocol, one-way repeated measures analysis of variance (ANOVA) followed by Dunnett's test was used to compare variables at each stimulation against the baseline value. The paired t test was used to compare variables between pedicled and skeletonized LITA grafts at each stimulation level. Linear regression analysis was used to examine the relationship between the double product and graft flow. Differences were considered to be significant at a threshold of $P < 0.05$.

Results

Prior to sympathetic stimulation, baseline graft flow (under spontaneous sympathetic outflow) was greater in skeletonized ITA than pedicled ITA (Table 1). Other

Table 1 Hemodynamic parameters and graft flow before stimulation

Hemodynamic parameters	Pedicled	Skeletonized	P value
Heart rate (beats/min)	104 ± 8	106 ± 8	NS
Mean arterial pressure (mmHg)	94 ± 7	93 ± 7	NS
Cardiac output (ml/min/kg)	83 ± 17	74 ± 9	NS
Double product (mmHg beats/min)	11368 ± 834	11346 ± 621	NS
Graft flow before stimulation (ml/min)	22.6 ± 2.7	27.8 ± 1.9	<0.05

Values are given as the mean $\pm$ standard error (SE)

NS Not significant

hemodynamic parameters, including heart rate, cardiac output, mean arterial pressure, and double product, did not differ significantly regardless of harvesting technique.

Graft flow patterns at baseline and under sympathetic stimulation are shown in Fig. 1a. Sympathetic stimulation increased graft flow ($P < 0.05$) similarly in skeletonized and pedicled ITA grafts, and maximal flow was comparable to each other at 10-Hz stimulation [nonsignificant (NS) difference] (Fig. 1b). Increases in systemic arterial pressure and heart rate did not differ significantly between the two techniques (Fig. 2), and increases in myocardial oxygen demand in response to sympathetic stimulation, as estimated by double product, were likewise similar.

Graft flow (y) correlated well with the double product (x) in both pedicled ($y = 2.6 \times 10^{-3}x - 8.4$, $R^2 = 0.73$) and skeletonized ITA ($y = 2.3 \times 10^{-3}x - 0.7$, $R^2 = 0.69$). The slope and y-intercept did not differ statistically between the two techniques (Fig. 3).

Discussion

The choice of either skeletonized or pedicled ITA grafts for CABG may be an important decision from both the technical and clinical viewpoints; however, clear evidence demonstrating the advantage of either method over the other is not yet available. In this study, we have shown that graft flow increased to a similar level during maximal sympathetic stimulation in both pedicled and skeletonized ITA grafts. These results do not support our hypothesis that the skeletonized ITA would provide larger flow capacity and indicate that coronary vasodilatation in response to increased myocardial oxygen demand is a stronger determinant of graft flow than any possible increase in the vascular resistance of ITA itself. Our study also demonstrates that both skeletonized and pedicled ITAs were able to supply adequate graft flow after CABG even during intense sympathoexcitation.

There are several possible explanations for the difference in graft flow under baseline conditions. First, a loss of sympathetic innervation in the skeletonized graft may have dilated the ITA relative to the pedicled graft under baseline conditions. In support of this explanation, Takami et al. [7] reported that the diameter of the ITA just proximal to the anastomosis is significantly larger in the skeletonized ITA than that in the pedicled ITA. Dönmez et al. [10] reported that the diameter of ITA becomes statically larger by the stellate ganglion blockade. In a preliminary study, we observed that electrical stimulation of the stellate ganglion decreased ITA flow before harvest. Therefore, vasoconstriction may occur in the pedicled ITA during sympathetic stimulation. However, in this study we did not perform simultaneous measurements of the graft flow and diameter

Fig. 1 **a** Typical representative recording of graft flow with pedicled and skeletonized internal thoracic arteries (*ITAs*) during sympathetic nerve stimulation. **b** Mean graft flow with pedicled (*closed circle*) and skeletonized (*open circle*) ITAs during sympathetic nerve stimulation. Data are shown as the mean $\pm$ standard error (SE). $^{\dagger}P < 0.05$ vs. baseline, $^{\ddagger}P < 0.01$ vs. baseline, $^{*}P < 0.05$ pedicled vs. skeletonized
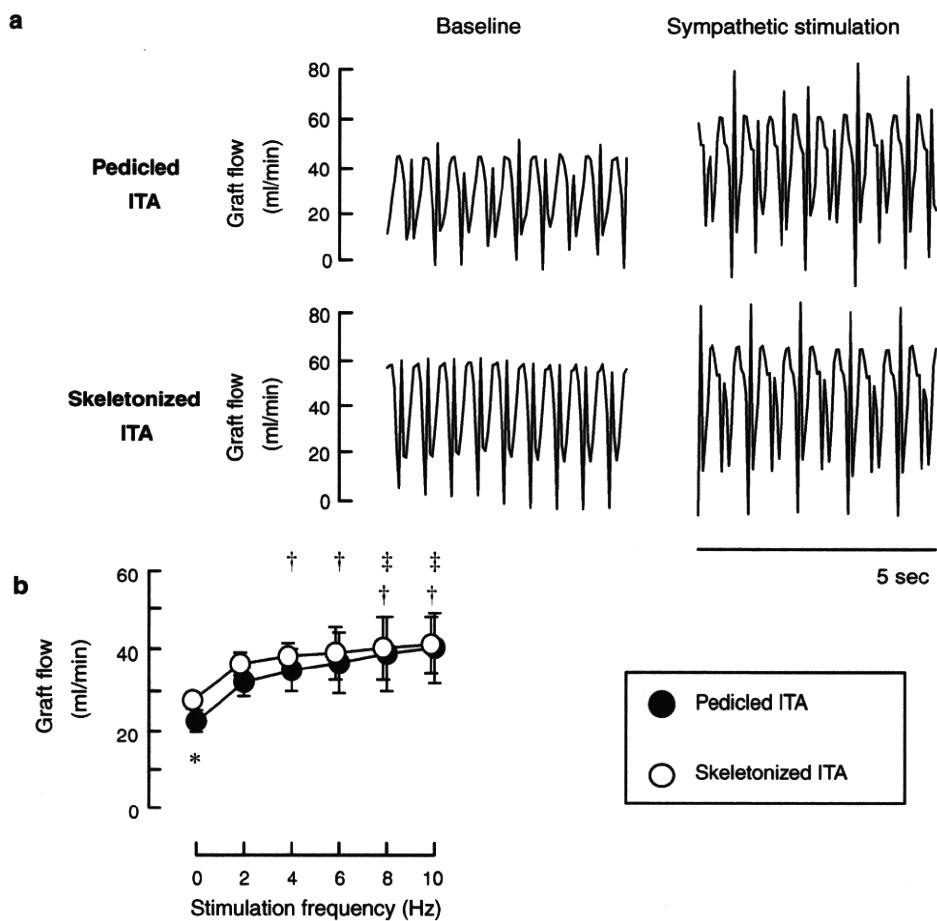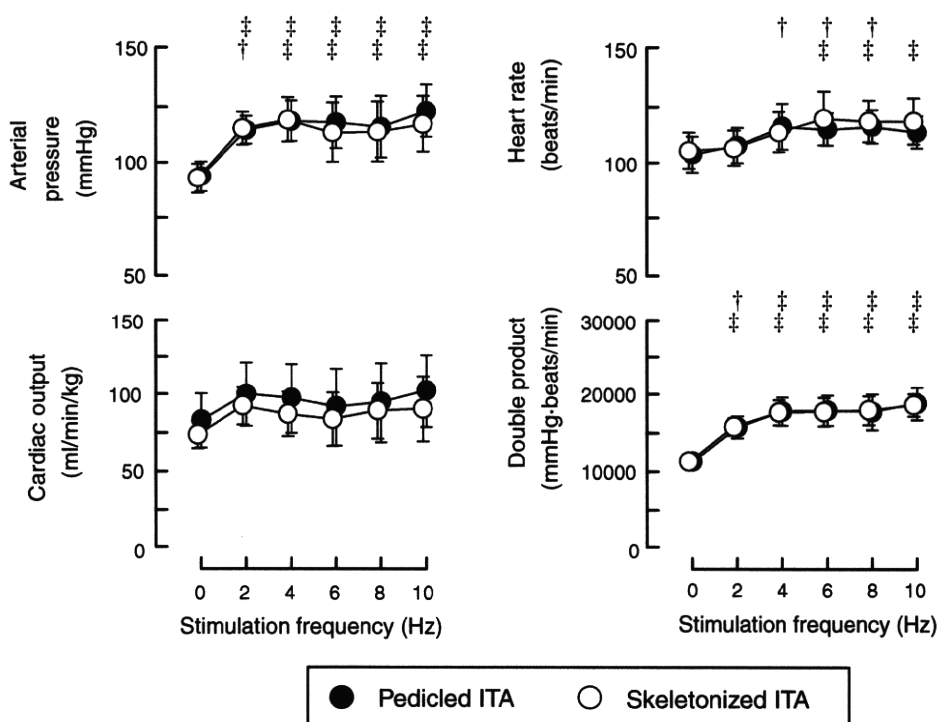

Fig. 2 Changes in mean arterial pressure, cardiac output, heart rate, and double product with pedicled (*closed circle*) and skeletonized (*open circle*) ITAs during sympathetic nerve stimulation. Data are shown as the mean $\pm$ SE. $^{\dagger}P < 0.05$ vs. baseline, $^{\ddagger}P < 0.01$ vs. baseline
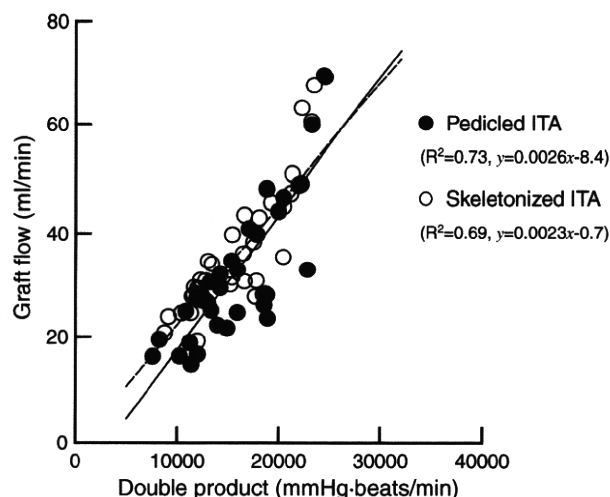

Fig. 3 Scatter plots and regressions between the double product and graft flow with pedicled (*closed circle, solid line*) and skeletonized (*open circle, dashed line*) ITAs. Regression lines did not differ between the two groups. *y* Graft flow, *x* double product

because the use of contrast medium in angiography may have affected the graft flow through its vasodilatative effect on the coronary artery [11].

Another explanation may be the difference in background sympathetic tone. As the skeletonized graft flow was always studied in the later phase of the experiment, when background sympathetic tone and myocardial metabolic demand may be higher, skeletonized graft flow may have been higher for this reason. The presence of similar hemodynamics during the two protocols, however, does not directly support this explanation. The hemodilution seen predominantly in the later phase of the experiment may also have contributed to higher flow through the skeletonized graft under baseline conditions.

The fact that graft flows were similar between the skeletonized and pedicled ITAs during maximal sympathetic excitation indicates that the resistance of the ITA graft was much smaller than that of the native coronary bed, even when the coronary bed was maximally dilated to meet the oxygen demand present with maximal sympathetic stimulation. In other words, both the skeletonized and pedicled ITAs would appear to provide sufficient flow reserve to the LAD area. In contrast, it has been reported that free flow, which may represent the maximal flow capacity of the ITA itself, is greater in the skeletonized ITA than in the pedicled ITA [2, 3]. Despite these previous findings, because the maximally dilated native coronary bed would be the most practical downstream conduit to test the difference between the skeletonized and pedicled ITAs, we believe that the difference in sympathetic innervation does not affect the maximal flow significantly under anastomosed conditions.

In addition to the effects of downstream resistance, local mechanisms would also contribute to the observed difference in flow between the pedicled and skeletonized ITA grafts. Complete sympathetic denervation with the local application of phenol to the skeletonized ITA further increased graft flow (unpublished observation), suggesting that there remains a certain sympathetic innervation in the skeletonized ITA. Even though sympathetic denervation may not be complete after skeletonization, we believe that our skeletonization did not differ greatly from those clinically performed by surgeons. Deja et al. [4] reported that skeletonization increases the reactivity of ITA to norepinephrine in vitro. Their study may support our results. Prior to sympathetic stimulation but under spontaneous sympathetic outflow, the amount of endogenous norepinephrine release to the skeletonized ITA may be relatively smaller than that to the pedicled ITA; as such, the sympathetic vasoconstriction would be negligible in the skeletonized ITA. This may explain the larger graft flow in the skeletonized ITA prior to sympathetic stimulation. Under maximal sympathetic stimulation, however, hyperreactivity to endogenous norepinephrine in the skeletonized ITA may cause the sympathetic vasoconstriction similar to that occurring in the pedicled ITA. This local mechanism may also partly account for why graft flow was comparable between the pedicled and skeletonized ITAs during maximal sympathetic stimulation. Although the results from several pharmacological studies suggest that norepinephrine-induced vasoconstriction does occur in the ITA [12, 13], there have been no reports assessing the tissue norepinephrine concentration of ITA during sympathetic stimulation. Further investigations are necessary to gain an understanding of the difference in norepinephrine reactivity between the pedicled and skeletonized ITAs.

Some publications have reported several advantages of the skeletonized ITA grafts other than the potential increase in graft flow at rest [1, 14]. Firstly, skeletonization lengthens the ITA, thereby providing access to more distal targets in the coronary artery [15]. Second, skeletonization improves blood supply to the sternum (measured by single photon emission computed tomography) [16] compared with pedicled harvesting. Third, skeletonization decreases the incidence of postoperative respiratory dysfunction because of less invasive harvesting (i.e., preserved pleural integrity in skeletonized ITA vs. pleurotomy in pedicled ITA) [17, 18]. Lastly, skeletonization markedly reduces anterior chest pain and dysesthesia 3 months after surgery [19]. In contrast to these advantages, skeletonization has the minor disadvantages of greater technical difficulty, longer harvesting duration, and potential damage to the graft.

Limitations

This study has several limitations. First, because skeletonized graft flow measurements always follow pedicled graft flow measurements in the same dog, the effect of time sequence on graft flows cannot be ruled out. Nevertheless, the similar hemodynamic response to sympathetic stimulation between protocol 1 and 2 (Fig. 2) suggests that the animal conditions did not deteriorate considerably. Second, the perfusion area of LITA was limited to the LAD region. If we had used a much larger perfusion area of LITA, the possible small difference between the pedicled and skeletonized ITAs may have been revealed. Third, a histological comparison between the pedicled and skeletonized ITA was not performed because the pedicled ITA was always skeletonized after the protocol 1, and the tissue samples from the pedicled ITA could not be obtained. Further investigations that include histological comparison are necessary for examining the effect of skeletonization on sympathetic innervations.

Conclusion

Both the pedicled and skeletonized ITA techniques supplied similar, adequate blood flow to the LAD, meeting myocardial oxygen demand during sympathetic excitation. Metabolic demand can override the possible difference in sympathetic vasoconstriction, increasing the flow in both pedicled and skeletonized ITA grafts to a similar extent when they are anastomosed to LAD. The results of this study have an important implication in terms of clinical application. Following anastomosis, graft flow is highly variable and is dependent on myocardial oxygen demand. Because the quality of CABG may be judged based on flow through anastomosed grafts, one has to take into consideration the potential change in flow in response to myocardial oxygen demand.

References

1. Del Campo C (2003) Pedicled or skeletonized? A review of the internal thoracic artery graft. Tex Heart Inst J 30:170–175
2. Castro GP, Dussin LH, Wender OB, Barbosa GV, Saadi EK (2005) Comparative analysis of the flows of left internal thoracic artery grafts dissected in the pedicled versus skeletonized manner for myocardial revascularization surgery. Arq Bras Cardiol 84:261–266
3. Deja MA, Woś S, Gołba KS, Zurek P, Domaradzki W, Bachowski R, Spyt TJ (1999) Intraoperative and laboratory evaluation of skeletonized versus pedicled internal thoracic artery. Ann Thorac Surg 68:2164–2168
4. Deja MA, Gołba KS, Malinowski M, Woś S, Kolowca M, Biernat J, Kajor M, Spyt TJ (2005) Skeletonization of internal thoracic artery affects its innervation and reactivity. Eur J Cardiothorac Surg 28:551–557
5. Wendler O, Tscholl D, Huang Q, Schäfers HJ (1999) Free flow capacity of skeletonized versus pedicled internal thoracic artery grafts in coronary artery bypass grafts. Eur J Cardiothorac Surg 15:247–250
6. Onorati F, Esposito A, Pezzo F, di Virgilio A, Mastroroberto P, Renzulli A (2007) Hospital outcome analysis after different techniques of left internal mammary grafts harvesting. Ann Thorac Surg 84:1912–1919
7. Takami Y, Ina H (2002) Effects of skeletonization on intraoperative flow and anastomosis diameter of internal thoracic arteries in coronary artery bypass grafting. Ann Thorac Surg 73:1441–1445
8. Austen WG, Edwards JE, Frye RL, Gensini GG, Gott VL, Griffith LS, McGoon DC, Murphy ML, Roe BB (1975) A reporting system on patients evaluated for coronary artery disease. Report of the Ad Hoc Committee for Grading of Coronary Artery Disease, Council on Cardiovascular Surgery, American Heart Association. Circulation 51:5–40
9. Kitamura K, Jorgensen CR, Gobel FL, Taylor HL, Wang Y (1972) Hemodynamic correlates of myocardial oxygen consumption during upright exercise. J Appl Physiol 32:516–522
10. Dönmez A, Tufan H, Tutar N, Araz C, Sezgin A, Karadeli E, Torgay A (2005) In vivo and in vitro effects of stellate ganglion blockade on radial and internal mammary arteries. J Cardiothorac Vasc Anesth 19:729–733
11. Baile EM, Paré PD, D'yachkova Y, Carere RG (1999) Effect of contrast media on coronary vascular resistance: contrast-induced coronary vasodilation. Chest 116:1039–1045
12. Evora PR, Pearson PJ, Discigil B, Oeltjen MR, Schaff HV (2002) Pharmacological studies on internal mammary artery bypass grafts. Action of endogenous and exogenous vasodilators and vasoconstrictors. J Cardiovasc Surg (Torino) 43:761–771
13. He GW, Yang CQ, Starr A (1995) Overview of the nature of vasoconstriction in arterial grafts for coronary operations. Ann Thorac Surg 59:676–683
14. Athanasiou T, Crossman MC, Asimakopoulos G, Cherian A, Weerasinghe A, Glenville B, Casula R (2004) Should the internal thoracic artery be skeletonized? Ann Thorac Surg 77:2238–2246
15. Higami T, Yamashita T, Nohara H, Iwahashi K, Shida T, Ogawa K (2001) Early results of coronary grafting using ultrasonically skeletonized internal thoracic arteries. Ann Thorac Surg 71:1224–1228
16. Cohen AJ, Lockman J, Lorberboym M, Bder O, Cohen N, Medalion B, Schachner A (1999) Assessment of sternal vascularity with single photon emission computed tomography after harvesting of the internal thoracic artery. J Thorac Cardiovasc Surg 118:496–502
17. Bonacchi M, Prifti E, Giunti G, Salica A, Frati G, Sani G (2001) Respiratory dysfunction after coronary artery bypass grafting employing bilateral internal mammary arteries: the influence of intact pleura. Eur J Cardiothorac Surg 19:827–833
18. Matsumoto M, Konishi Y, Miwa S, Minakata K (1997) Effect of different methods of internal thoracic artery harvest on pulmonary function. Ann Thorac Surg 63:653–655

19. Boodhwani M, Lam BK, Nathan HJ, Mesana TG, Ruel M, Zeng W, Sellke FW, Rubens FD (2006) Skeletonized internal thoracic artery harvest reduces pain and dysesthesia and improves sternal perfusion after coronary artery bypass surgery: a randomized, double-blind, within-patient comparison. Circulation 114:766–773

Augmented ST-Segment Elevation During Recovery From Exercise Predicts Cardiac Events in Patients With Brugada Syndrome

Hisaki Makimoto, MD,* Eiichiro Nakagawa, MD, PHD,† Hiroshi Takaki, MD, PHD,*
Yuko Yamada MD,* Hideo Okamura, MD,* Takashi Noda, MD, PHD,* Kazuhiro Satomi, MD, PHD,*
Kazuhiro Suyama, MD, PHD,* Naohiko Aihara, MD,* Takashi Kurita, MD, PHD,‡
Shiro Kamakura, MD, PHD,* Wataru Shimizu, MD, PHD*

Suita and Osaka, Japan

Objectives	The goal of this study was to evaluate the prevalence and the clinical significance of ST-segment elevation during recovery from exercise testing.
Background	During recovery from exercise testing, ST-segment elevation is reported in some patients with Brugada syndrome (BrS).
Methods	Treadmill exercise testing was conducted for 93 patients (91 men), 46 ± 14 years of age, with BrS (22 documented ventricular fibrillation, 35 syncope alone, and 36 asymptomatic); and for 102 healthy control subjects (97 men), 46 ± 17 years of age. Patients were routinely followed up. The clinical end point was defined as the occurrence of sudden cardiac death, ventricular fibrillation, or sustained ventricular tachyarrhythmia.
Results	Augmentation of ST-segment elevation ≥0.05 mV in V_1 to V_3 leads compared with baseline was observed at early recovery (1 to 4 min at recovery) in 34 BrS patients (37% [group 1]), but was not observed in the remaining 59 BrS patients (63% [group 2]) or in the 102 control subjects. During 76 ± 38 months of follow-up, ventricular fibrillation occurred more frequently in group 1 (15 of 34, 44%) than in group 2 (10 of 59, 17%; p = 0.004). Multivariate Cox regression analysis showed that in addition to previous episodes of ventricular fibrillation (p = 0.005), augmentation of ST-segment elevation at early recovery was a significant and independent predictor for cardiac events (p = 0.007), especially among patients with history of syncope alone (6 of 12 [50%] in group 1 vs. 3 of 23 [13%] in group 2) and among asymptomatic patients (3 of 15 [20%] in group 1 vs. 0 of 21 [0%] in group 2).
Conclusions	Augmentation of ST-segment elevation during recovery from exercise testing was specific in patients with BrS, and can be a predictor of poor prognosis, especially for patients with syncope alone and for asymptomatic patients. (J Am Coll Cardiol 2010;56:1576–84) © 2010 by the American College of Cardiology Foundation

Brugada syndrome (BrS) is recognized as a clinical syndrome that leads to sudden cardiac death (SCD) in middle-aged persons due to ventricular fibrillation (VF) (1). Brugada syndrome is defined by a distinct 12-lead electrocardiogram (ECG) pattern in precordial leads (V_1 to V_3) presenting coved-type ST-segment elevation. Both depolar-

ization and repolarization hypotheses have been reported for the pathogenesis of phenotype in BrS (2–5). Although several indexes have been reported as predictive factors of VF occurrence (6), the recent largest series of BrS patients suggested that there were no reliable predictors of cardiac events except for prior symptoms and spontaneous type 1 ECG (7). However, risk stratification remains disputable, especially for BrS patients without documented VF episodes.

Autonomic function has been suggested to relate to the occurrence of VF in BrS. It has also been shown that ST-segment elevation in patients with BrS was augmented

by selective stimulation of muscarinic receptors but miti-
gated by beta-adrenergic stimulation (8). Heart rate during
exercise testing is considered as 1 parameter to evaluate
cardiac autonomic function (9). Sympathetic withdrawal
and parasympathetic activation occur at early recovery after
exercise (10), which are expected to augment ST-segment
elevation directly by inhibition of calcium-channel current
or by decreasing heart rate (5,11). Two cases of BrS were
reported in which ST-segment was augmented during and
after exercise (12). Amin et al. (13) recently assessed the
ECG responses to exercise in BrS patients with and without
SCN5A mutations and control subjects. They reported that
exercise resulted in an increase of peak J-point amplitude in
all groups, including control subjects, and more QRS
widening in BrS patients with *SCN5A* mutation. The peak
J-point amplitude measured by Amin et al. (13) is thought
to represent the depolarization parameter as QRS duration,
or at least the combined parameter of both depolarization
and repolarization. Therefore, in the present study, we
measured several points of ST-segment as a repolarization
parameter rather than a depolarization parameter, and tried
to investigate the relationship between augmented ST-
segment elevation during recovery from exercise testing and
prognosis of BrS patients. We also evaluated parasympa-
thetic reactivation by using heart rate recovery (HRR),
which is defined as heart rate decay in the first minute after
exercise cessation, and its relation with ST-segment change.

Methods

Study population. The study population consisted of 93
consecutive Japanese patients with BrS (91 males; mean age
46 ± 14 years) admitted to the National Cerebral and
Cardiovascular Center in Suita, Japan, between 1994 and
2006. Ventricular fibrillation was documented in 22 BrS
patients, syncope alone in 35 patients, and the remaining 36
patients were asymptomatic. As control subjects, 102 age-,
sex-, and QRS duration-matched healthy subjects were
randomly selected from persons who underwent treadmill
exercise testing between 2002 and 2007 (97 males; mean age
46 ± 17 years). They included 55 normal subjects with
normal QRS duration (<100 ms), 21 with incomplete right
bundle branch block (RBBB) (100 ms ≤QRS duration
<120 ms), and 26 with complete RBBB (120 ms ≤QRS
duration) but without structural heart disease or any ven-
tricular arrhythmias.

Brugada syndrome was diagnosed when a coved ST-
segment elevation (≥0.2 mV at J-point) was observed in >1 of
the right precordial leads (V_1 to V_3) in the presence or absence
of a sodium-channel–blocking agent, and in conjugation with
1 of the following: documented VF, polymorphic ventricular
tachycardia, family history of SCD <45 years of age, family
history of BrS, inducibility of VF with programmed electrical
stimulation, syncope, or an nocturnal agonal respiration (6).
Structural heart diseases were carefully excluded by history

taking, physical examinations,
chest roentgenogram, ECG, and
echocardiogram.
**Clinical, laboratory, electrocar-
diographic, and electrophysi-
ologic study.** The following clin-
ical data were collected: family
history of SCD (<45 years of age)
or BrS, documented atrial fibrilla-
tion (AF), documented VF, syn-
cope, age at the first cardiac event,
and implantation of implantable
cardioverter-defibrillator (ICD).

A 12-lead ECG was recorded
in all 93 BrS patients, and RR
interval, PR interval (lead II),
QRS duration (lead V_5), cor-
rected QT interval (lead V_2),
QRS axis, J-point amplitude
(leads V_2), and amplitude of several points of ST-segment
(leads V_1, V_2, V_3) were measured.

Signal-averaged ECG was recorded and analyzed in
91 patients by using a signal-averaged ECG system
(1200EPX, Arrhythmia Research Technology, Milwaukee,
Wisconsin). Three parameters were assessed using a com-
puter algorithm: 1) total filtered QRS duration; 2) root
mean square voltage of the terminal 40 ms of the filtered
QRS complexes (V_{40}); and 3) duration of low-amplitude
signals <40 μV of the filtered QRS complexes (T_{40}). Late
potential was considered present when the 2 criteria (V_{40}
<18 μV and T_{40} >38 ms) were fulfilled.

Electrophysiologic study (EPS) was performed in 79 BrS
patients (21 documented VF patients, 30 syncope alone
patients, and 28 asymptomatic patients). A maximum of 3
programmed ventricular extrastimuli were delivered from
the right ventricular apex and RVOT, unless VF was
induced. No patients received antiarrhythmic drugs before
EPS. The atrio-His and His-ventricular intervals were
measured during sinus rhythm. The EPS was conducted
after all subjects gave written informed consent.

Genetic testing for the presence of an *SCN5A* mutation
was also conducted.
Exercise testing. Treadmill exercise testing was conducted
in all 93 patients with BrS and 102 control subjects. Neither
BrS patients nor control subjects used antiarrhythmic
agents. A symptom-limited or submaximal (up to 90% of
the age-predicted maximum heart rate) graded treadmill
exercise testing similar to modified Bruce protocol was used.
All 93 BrS patients and 102 control subjects were in normal
sinus rhythm, and none had atrioventricular block at the
exercise testing. The standard 12-lead ECGs were recorded
at rest, at the end of each exercise stage, at peak exercise, and
at every minute during recovery. The amplitude of ST-
segment from the isoelectric line at the right precordial leads
(V_1 to V_3 leads) and QRS width at V_5 lead were manually
measured. The ST-segment point was defined as the point

where the vertical line from the end point of QRS at V_5 lead intersected the precordial leads. We also measured peak J-point amplitude in lead V_2 as a depolarization parameter, and amplitude of the point, which was 40 and 80 ms later than the peak J-points (ST40, ST80) in lead V_2 as a repolarization parameter. Measurements of ECG parameters were performed as the mean of 3 beats by single electrocardiologist who knew nothing about the patients. Significant augmentation of ST-segment elevation was defined as ST-segment amplitude increase ≥ 0.05 mV in at least 1 of V_1 to V_3 leads at early recovery (1 to 4 min at recovery) compared with the ST-segment amplitude at baseline (pre-exercise). We also recorded heart rate and blood pressure during exercise testing.

The HRR was defined as decay of heart rate from peak exercise to 1 min at recovery.

Follow-up. Follow-up was started after undergoing treadmill exercise testing. All patients with BrS were routinely followed up at the outpatient clinic of our hospital. The ICD implantation was performed in 63 BrS patients (20 documented VF patients, 25 syncope alone patients, and 18 asymptomatic patients). Antiarrhythmic drugs were prescribed for 7 patients; 2 patients who had episodes of VF but refused implantation of ICD (disopyramide 300 mg daily for 1 patient, and amiodarone 200 mg daily for another patient), 2 patients who had AF (quinidine 300 mg daily), and 3 patients who had previous history of both VF and AF and implanted ICD (quinidine 300 mg daily for 1 patient, amiodarone 200 mg daily for 2 patients).

Cardiac events were defined as SCD or aborted cardiac arrest, and VF or sustained ventricular tachyarrhythmia documented by ICD or ECG recordings.

Statistical analysis. Data were analyzed with Dr. SPSS II for Windows software package (SPSS Inc., Chicago, Illinois). Numeric values are expressed as mean ± SD. The chi-square test, Student t test, or 1-way analysis of variance was performed when appropriate to test for statistical differences. All p values <0.05 were considered statistically significant. Event rate curves were plotted according to the Kaplan-Meier method, and were analyzed with the log-rank test. Univariate and multivariate Cox regression were performed to assess whether 7 indexes can be significant and independent predictors of subsequent cardiac events. We used the forward step-wise approach with p to enter a value of 0.05 for multivariate analysis. Augmentation of ST-segment elevation at early recovery, family history of SCD or BrS, spontaneous coved-type ST-segment elevation, presence of *SCN5A* mutation, late potential, VF inducibility during EPS, and previous episodes of VF were included as indexes.

Results

There were no significant differences between 93 BrS patients and 102 control subjects with respect to age at

Table 1	Initial Characteristics of Patients and Control Subjects		
	Brugada Patients (n = 93)	Control Subjects (n = 102)	p Value
Age at exercise testing, yrs	46 ± 14	46 ± 17	NS
Sex, male	91 (98%)	97 (95%)	NS
Electrocardiographic characteristics, ms			
RR	952 ± 151	903 ± 140	0.020
PR	178 ± 30	165 ± 24	0.001
QRS duration	98 ± 16	98 ± 20	NS
QTc	416 ± 44	406 ± 30	NS

Values are mean ± SD or n (%).
QTc = corrected QT interval.

exercise testing, sex, QRS duration (lead V_5), and QTc interval (lead V_2), as summarized in Table 1. The RR interval and PR interval (lead II) were significantly longer in BrS patients than in control subjects.

Response of ST-segment elevation during treadmill exercise testing. Among 93 BrS patients, significant augmentation of ST-segment elevation mostly associated with coved pattern at early recovery phase was observed in 34 BrS patients (37% [group 1]), but not in the remaining 59 BrS patients (63% [group 2]). Conversely, ST-segment augmentation was never observed in any of the 102 control subjects (34 of 93 [37%] vs. 0 of 102 [0%], p < 0.0001). Typical responses of ST-segment amplitudes of 3 groups are shown in Figure 1. Composite data of serial changes of ST-segment amplitude in V_1 and V_2 leads during exercise testing are illustrated in Figure 2A. The serial changes of ST-segment amplitude in V_3 lead showed the same trend (not shown). In group 1, ST-segment amplitude decreased at peak exercise and started to reascend at early recovery, and culminated at 3 min of recovery (Figs. 1A and 2A). In contrast, ST-segment amplitude of group 2 patients and control subjects decreased at peak exercise, and gradually returned to the baseline amplitude rather than showing augmentation (Figs. 1B to 1D and 2A). Significant differences were identified between group 1 and group 2 patients in the ST-segment amplitude in leads V_1 and V_2 from peak exercise to 6 min of recovery, whereas no major differences were observed between group 2 patients and control subjects (Fig. 2A). Composite data of serial changes of peak J-point amplitude, ST40, and ST80 amplitudes are presented in Figure 2B. The peak J-point amplitude and ST40 amplitude during recovery showed the same trend as the ST-segment amplitude in Figure 2A. Significant differences were identified between group 1 and group 2 patients in the peak J-point and ST40 amplitudes from peak exercise to 6 min of recovery. The ST80 amplitude showed significant differences between group 1 and group 2 patients at 2, 3, and 4 min of recovery. At peak exercise, the peak J-point amplitude increased in 34 (37%) of 93 Brugada patients and in 26 (26%) of 102 control subjects, although the ST-segment